PURBANCHAL UNIVERSITY

KHWOPA ENGINEERING COLLEGE

DEPARTMENT OF ELECTRONIC COMMUNICATION AND

AUTOMATION ENGINEERING

LIBALI-8, BHAKTAPUR

DUAL-AXIS SOLAR TRACKER WITH INVERTER FOR EFFICIENT SOLAR ENERGY CONVERSION

(COURSE CODE: BEC8031)

A Final report

Submitted by

BHAGWAN KARKI (780403)

DEBAKI SHRESTHA (780404)

PALDEN NHORU TAMANG (780408)

In partial fulfillment for the award of the degree of

BACHELOR DEGREE OF ELECTRONICS COMMUNICATION

AND AUTOMATION ENGINEERING

July, 2026

BONAFIDE CERTIFICATE

The undersigned certify that this final year project titled **"DUAL-AXIS SOLAR TRACKER WITH INVERTER FOR EFFICIENT SOLAR ENERGY CONVERSION"** is the bonafide work of **Bhagwan Karki (780403), Debaki Shrestha (780404), and Palden Nhoru Tamang (780408),** for the partial fulfillment of the degree of Bachelor in Electronics, Communication and Automation Engineering

....

Er. Gaurab Tamrakar

Supervisor

Lecturer

Khwopa College of Engineering

....

Er. Yogesh Bajracharya

Supervisor

Associate Professor

Khwopa Engineering College

....

Er. Yogesh Bajracharya

Head of Department

Department of Electronics Communication and Automation Engineering

....

Er. Debendra Bahadur Raut

External Examiner

Assistant Professor

Department of Automobile and Mechanical Engineering

Institute of Engineering, Thapathali Campus

Tribhuvan University

ACKNOWLEDGEMENT

We would like to express our sincere gratitude to our project supervisors **Er. Gaurav Tamrakar** and **Er Yogesh Bajracharya** for their continuous guidance, encouragement, and valuable suggestions throughout the development of this project. Their technical insights and constructive feedback played a crucial role in shaping the successful completion of the final phase.

We would also like to thank the faculty members of the Department of Electronics, Communication, and Automation Engineering for providing the necessary academic support, laboratory facilities, and learning environment required for this project. We also sincerely thank **Mr. Shiva Ram Awal** and **Mr. Rajendra Kasula** for their resource facilitation. Our heartfelt appreciation goes to our college administration for offering the resources and infrastructure needed for practical implementation.

Our heartfelt thanks go to our **friends and colleagues** for their unwavering patience, motivation, and moral support, which kept us encouraged and focused throughout this challenging journey.

Finally, we acknowledge the **open-source communities and technical contributors** whose work, libraries, and documentation greatly facilitated our development process.

This project would not have been possible without the collective support of everyone mentioned above.

Thank You.

Bhagwan Karki (780403)

Debaki Shrestha (780404)

Palden Nhoru Tamang (780408)

ABSTRACT

Fixed-orientation solar panels lose a significant portion of available solar energy because their alignment does not adjust to the sun's changing position throughout the day. This project addresses that limitation through the design and implementation of a standalone Dual-Axis Solar Tracker with an Inverter for Efficient Solar Energy Conversion. The system uses an ESP32 microcontroller to continuously adjust the solar panel's orientation along both azimuth and elevation axes via two stepper motors driven by TB6600 drivers, based on solar position calculations referenced to a real-time clock and fixed geographic coordinates. Energy harvested by the panel is regulated and stored in a 12V, 60Ah lead-acid battery system, and a push-pull inverter converts the stored DC power into AC for standalone loads. Key electrical parameters, panel voltage, current, power, and energy are continuously monitored using calibrated current and voltage sensors, with data logged to an SD card and displayed through a real-time web dashboard hosted on the ESP32's built-in Wi-Fi access point, which also allows manual override of tracking angles. To evaluate the system's effectiveness, the dual-axis tracker and a fixed static panel were tested simultaneously under identical conditions, with measurements recorded every three minutes over a six-hour session (10:00–16:00). Results showed the dual-axis tracker achieved approximately a 32.0% higher average power output, a 32.2% greater total energy yield, and an 8.0% higher peak power output compared to the static panel, when a fixed panel's misalignment with the sun is greatest. These results confirm that active dual-axis tracking, combined with integrated monitoring and inverter-based power delivery, meaningfully improves the utilization of solar energy over conventional fixed-panel systems, offering a low-cost and reliable solution suitable for standalone applications under Nepal's geographical and climatic conditions.

Keywords: Dual-Axis Solar Tracker, ESP32, Solar Position Algorithm, Stepper Motor Control, Standalone Inverter, Renewable Energy, Solar Energy Monitoring.

TABLE OF CONTENTS

LIST OF FIGURES

ABBREVIATIONS

AC – Alternating Current

DC – Direct Current

ESP32 – Espressif Systems 32-bit Microcontroller

GPS – Global Positioning System

I2C – Inter-Integrated Circuit

IEC – International Electrotechnical Commission

IEEE – Institute of Electrical and Electronics Engineers

IoT – Internet of Things

LCD – Liquid Crystal Display

LED – Light Emitting Diode

MCPWM - Motor Control PWM (ESP32 peripheral)

MPPT – Maximum Power Point Tracking

NEMA – National Electrical Manufacturers Association

PCB – Printed Circuit Board

PV – Photovoltaic

PWM – Pulse Width Modulation

RTC – Real-Time Clock

SoC – State of Charge

SPA – Solar Position Algorithm

SPWM - Sinusoidal Pulse Width Modulation

THD – Total Harmonic Distortion

Wi-Fi – Wireless Fidelity

CHAPTER 1: INTRODUCTION

1.1 Background

With the increasing demand for reliable and uninterrupted electrical power, renewable energy systems, particularly solar energy, are being widely adopted as an alternative to conventional energy sources. Solar energy is clean, renewable, and environmentally friendly; however, the power output of traditional fixed solar panel systems is highly dependent on the sun's position, weather conditions, and daylight duration. Due to fixed panel orientation, a considerable amount of available solar energy is not efficiently utilized.

To overcome this limitation, solar tracking systems are employed to improve energy harvesting efficiency. A dual-axis solar tracking system continuously adjusts the orientation of the solar panel in azimuth and elevation directions, ensuring maximum exposure to sunlight throughout the day and across seasonal variations. Compared to fixed-tilt systems, dual-axis tracking significantly increases energy generation.

This project focuses on the design and development of a standalone **Dual-Axis Solar Tracker with Inverter for Efficient Solar Energy Conversion** using basic power electronics and embedded control. The system utilizes light sensors and a microcontroller-based control unit to detect the sun's position and automatically control two independent motors for precise panel alignment.

The electrical energy generated by the solar panel is directly regulated using a conventional charge control and voltage regulation circuit and stored in a battery system. An inverter is then used to convert the stored DC power into AC power for standalone loads. Continuous monitoring of key electrical parameters such as panel voltage, battery voltage, and load current ensures safe and reliable operation of the system.

By integrating dual-axis solar tracking with a simple inverter and battery-based power management, the proposed system enhances overall solar energy utilization while maintaining low system complexity and cost. This makes the system suitable for standalone solar applications and academic prototype development under Nepal's geographical and climatic conditions.

1.2 Problem Statement

Many conventional standalone solar inverter systems rely on fixed-position solar panels without automated tracking mechanisms. Due to the continuous variation in the sun's trajectory across the day and seasons, static panels fail to maintain optimal solar alignment, leading to significant energy yield losses and inefficient power generation. Consequently, such systems depend heavily on battery storage, causing deeper discharge cycles, reduced battery lifespans, and compromised system reliability. Furthermore, many small-scale installations lack integrated real-time monitoring and dynamic protection mechanisms, leaving them vulnerable to over-voltage, under-voltage, and over-current faults.

1.3 Objectives

Main Objective:

To design and implement a Dual-Axis Solar Tracker with an Inverter for Efficient Solar Energy Conversion.

Specific Objectives:

- To design and implement a dual-axis solar tracking system that continuously aligns the solar panel along azimuth and elevation axes to maximize solar energy capture.
- To develop a microcontroller-based control unit for processing sensor data and controlling the motors used in the dual-axis tracking mechanism.
- To design and implement a standalone solar inverter system that converts DC power from the solar panel–battery system into AC power for loads.
- To conduct experimental data acquisition and performance analysis by measuring solar panel voltage, current, power output, and energy generation, and comparing the results with a fixed solar panel system to evaluate efficiency improvements.
- To implement a web-based dashboard monitoring system that enables real-time acquisition and visualization of system parameters.

1.4 Scope and Limitations of the Study

Scope

- **Higher solar energy generation** – Tracking maximizes sunlight capture.
- **Reduced grid dependency** – More solar energy means less reliance on unstable electricity.
- **Efficient energy management** – Microcontroller control prevents energy waste.
- **Reliable AC output** – Provides stable power for small-scale/domestic use.

Limitations

- The system is intended for small-scale applications and is not suitable for high-power or utility-scale solar installations.
- The energy consumed by the tracking motors slightly reduces the net energy gain achieved through solar tracking, particularly under low irradiance conditions.
- Maximum Power Point Tracking (MPPT) is not implemented in the current system.
- The inverter system does not support grid-tied or hybrid operation.
- The system relies on accurate timekeeping and fixed geographical coordinates; errors in time synchronization or location data can impact tracking accuracy.

CHAPTER 2: LITERATURE REVIEW

The increasing demand for reliable, efficient, and sustainable electrical energy has accelerated the adoption of solar power systems, particularly in regions where conventional electricity supply is inconsistent. In Nepal, frequent power fluctuations, voltage instability, and limited grid reliability in rural and semi-urban areas highlight the need for intelligent solar-based power solutions capable of ensuring an uninterrupted electricity supply. An inverter-based solar power system with automatic source control provides an effective approach to addressing these challenges.

Dual-axis solar tracking systems have been extensively researched for their ability to significantly increase energy capture compared to fixed installations. Mousazadeh et al. [1] conducted a comprehensive review of sun-tracking methods, concluding that dual-axis systems can improve energy yield by 30–45% depending on geographic location. Their analysis of 52 studies showed that the performance improvement is particularly pronounced in regions with higher latitude variations, where the sun's path varies significantly throughout the year. For mechanical implementation, K. K. Chong and C. W. Wong [2] designed and tested a dual-axis tracker using stepper motors, achieving 40% energy gain over fixed systems. Their research emphasized the importance of backlash minimization in transmission systems for maintaining precise panel alignment. The study demonstrated that timing belt drives provide smoother operation compared to gear-based systems, with vibration reduction of up to 60%.

The Solar Position Algorithm (SPA) developed by I. Reda and A. Andreas [3] at the National Renewable Energy Laboratory provides the mathematical foundation for sensorless solar tracking. This algorithm calculates solar position with an accuracy of ±0.0003° using astronomical equations based on time, date, and geographic coordinates. The implementation eliminates weather dependency and provides consistent performance regardless of atmospheric conditions. For embedded system implementation, F. González-Longatt et al. [4] published a simplified solar position algorithm specifically designed for control systems. Their implementation on microcontrollers demonstrated that solar position calculations can be executed with minimal computational resources, requiring less than 4KB of RAM and completing within 100ms on 80MHz processors.

For stand-alone photovoltaic systems under 500W, specific inverter topologies have been optimized for reliability and efficiency. Y. Chen and K. M. Smedley [5] developed a cost-effective single-stage inverter with pure sine wave output, achieving efficiencies of 85–90% at full load for 100W systems. Their research demonstrated that H-bridge configurations with unipolar PWM modulation provide optimal performance for low-power applications. The IEEE Standard 1547-2018 [6] provides technical specifications for power conversion systems, including requirements for voltage regulation (±5% of nominal voltage), frequency stability (±0.5 Hz), and harmonic distortion limits (<5% total harmonic distortion). These standards ensure the reliable operation of stand-alone inverter systems. Safety requirements for solar power conversion systems are addressed in IEC 62109-1:2010 [7], which specifies protection mechanisms against electrical hazards. The standard requires overvoltage protection (15.5V cutoff for 12V systems), undervoltage protection (10.5V cutoff), and overcurrent protection with foldback characteristics, short-circuit protection with automatic reset, and thermal protection with derating capability. B. Singh et al. [8] implemented a microcontroller-based protection system that provides graduated response levels, from warning indicators to complete shutdown, based on fault severity. Their system incorporates temperature compensation and adaptive parameters based on operating conditions.

Monitoring systems play a crucial role in solar energy applications. K. T. Lee et al. [9] implemented an IoT-based solar monitoring system using ESP32, demonstrating real-time parameter tracking with web-based visualization. Their system monitored solar voltage, battery state of charge, inverter output, and panel orientation with update rates of 1 second.

Analysis and Testing of Dual-Axis Solar Tracker for Standalone Systems M. B. Prakash and K. Govindarajulu [10], this study focuses on the application of an automated dual-axis solar tracking system designed to maximize solar energy collection. The system integrates motorized mechanical structures, solar sensors, and a microcontroller-based control unit to continuously orient the photovoltaic panel toward the Sun. Experimental results show that, compared to fixed solar panels, the proposed tracking system achieved a significant increase in energy output, typically in the range of 31–42%. The study concludes that dual-axis solar trackers offer a highly effective approach for enhancing solar energy harvesting, as they are considerably more efficient than static systems in responding to the Sun’s position. Several studies have analyzed the control and performance of single-axis and dual-axis solar tracking systems with the objective of improving photovoltaic energy conversion efficiency without relying on light-based sensors.

In *Control of Single-Axis and Dual-Axis Solar Tracking System*, Taha, Mohamed, Abdulsalam, and Taha [11] focused on the control and performance analysis of Single-Axis Solar Tracking (SAST) and Dual-Axis Solar Tracking (DAST) systems. Arduino was used as the main control platform, while MATLAB/SIMULINK was employed for modeling and simulation. The study demonstrated that dual-axis tracking provides higher energy output and improved system stability compared to single-axis and fixed solar panel systems.

Various types of power inverters are discussed by Dileep D. K. and Bharath K. R. [12], including current-source and voltage-source inverters, stand-alone inverters, as well as square wave, modified sine wave and pure sine wave inverters. An open-loop control strategy is employed for MATLAB simulation of different Pulse Width Modulation (PWM) inverter techniques. The study also provides a brief explanation of the battery, charge controller, and photovoltaic (PV) array. Furthermore, different PWM techniques are compared based on cost, size, load type, and application, highlighting the suitability of stand-alone inverter systems for domestic and small-scale applications.

Biju K. and Ramchand R. [13] presented the design of a single-phase photovoltaic inverter system intended for standalone operation. A DC–DC boost converter is used to regulate the DC-link voltage obtained from the PV array. The inverter employs a Sinusoidal Pulse Width Modulation (SPWM) technique with a Proportional–Integral (PI) controller to regulate the output voltage supplied to the load. MATLAB/Simulink is used to simulate the system under various operating conditions, and the results demonstrate stable inverter performance for different load scenarios.

The design and fabrication of a custom Printed Circuit Board (PCB) is a critical step in transitioning an embedded solar tracking system from breadboard prototype to a reliable, deployable hardware. Vega-Durán et al. [14] designed and implemented a custom PCB for an embedded solar tracking control system, demonstrating that PCB-level integration of microcontrollers, motor drivers, and sensors significantly reduces wiring complexity and signal noise compared to breadboard assemblies. Their work highlighted that a dedicated PCB improves system compactness, mechanical stability, and long-term reliability under outdoor operating conditions. Gupta et al. [15] further investigated ESP32-based custom PCB design for IoT-enabled sensor fusion in solar energy applications, reporting a 35% reduction in noise-induced measurement errors and improved thermal management of power components. These findings are directly applicable to the 8th semester objective of this project, where a custom PCB will be fabricated to integrate the ESP32 microcontroller, stepper motor drivers, voltage and current sensors, and power management components into a single compact board for the dual-axis solar tracker system.

Nayak and Krishnamurthy [16] extended this approach by integrating cloud-based visualization with automated alert systems, enabling real-time notifications for over-voltage, under-voltage, and battery state-of-charge anomalies in standalone PV installations. K. T. Lee et al. [9], already cited in this review, further validated that ESP32-based IoT data acquisition at one-second update intervals provides sufficient temporal resolution for meaningful performance analysis of solar inverter systems. In this project, an IoT-based monitoring subsystem will be implemented using the ESP32 microcontroller to enable real-time acquisition and cloud-based visualization of key parameters including solar panel voltage, current, power output, battery state of charge, and inverter output, supporting both operational monitoring and systematic performance evaluation.

System performance optimization is essential for maximizing the net energy gain of a dual-axis solar tracking system while minimizing parasitic power losses from tracking motors and peripheral components. Abdallah and Nijmeh [17] conducted experimental studies on a two-axis solar tracking system, demonstrating that optimizing the tracking update interval and motor control logic can reduce unnecessary motor movements by up to 60%, thereby significantly lowering the energy consumed by the tracking mechanism without compromising alignment accuracy. Suresh and Venugopal [18] investigated dynamic power budgeting techniques in ESP32-based solar systems, showing that intelligent duty-cycling of peripheral components such as sensors and display modules can extend battery runtime by 18–22% under low-irradiance conditions.

Experimental data acquisition and performance analysis are fundamental to quantitatively validating the improvements achieved by a dual-axis solar tracking system over a fixed-panel installation. Islam et al. [19] conducted field measurements comparing fixed and dual-axis tracked photovoltaic panels, recording solar panel voltage, current, and power output at five-minute intervals over 30 days, confirming that dual-axis tracking yielded an average energy gain of 32.7% over fixed installations with peak gains exceeding 40%

during equinox periods. Seme et al. [20] further demonstrated that integrating cumulative energy logging with real-time power measurements, while accounting for tracking motor energy consumption, provides a comprehensive dataset for evaluating the true net efficiency of two-axis sun tracking systems. In this project, experimental data acquisition will be performed by measuring solar panel voltage, current, power output, and daily energy generation using the ACS712 current sensor and voltage divider circuits interfaced with the ESP32, enabling a direct quantitative comparison between the dual-axis tracked system and an equivalent fixed-panel configuration.

While substantial research exists on individual components of solar tracking systems, limited work addresses the complete integration of algorithm-based tracking with stand-alone inverter systems for small-scale applications. Specifically, there is insufficient documentation on the practical implementation of SPA on resource-constrained microcontrollers, mechanical design optimization for small-scale dual-axis trackers, integration strategies for monitoring and protection systems, and cost-performance optimization for educational applications. For Nepal specifically, additional challenges include adapting systems to variable voltage conditions (180-250V), designing for monsoon-resilient operation, and creating solutions that use locally available components and maintenance skills. This project contributes by addressing identified research gaps through the complete implementation of an algorithm-based tracking system without LDR sensors, detailed mechanical design using accessible components, full integration with a 100W stand-alone inverter system, comprehensive monitoring and protection implementation, and complete documentation suitable for replication and further development.

CHAPTER 3: METHODOLOGY

This chapter describes the overall design, development, and implementation procedure of the Dual-Axis Solar Tracker with Inverter for Efficient Solar Energy Conversion. It explains the system architecture, hardware and software integration, control algorithm, and testing approach adopted in this project. The methodology includes block diagram representation, algorithm development for sun tracking, inverter design, component selection, and system integration. The complete system is divided into major subsystems: solar tracking mechanism, power management and storage, inverter unit, monitoring and protection system, and control unit. Each subsystem was designed and tested individually before final integration to ensure reliable and efficient operation.

3.1 Block Diagram & Description

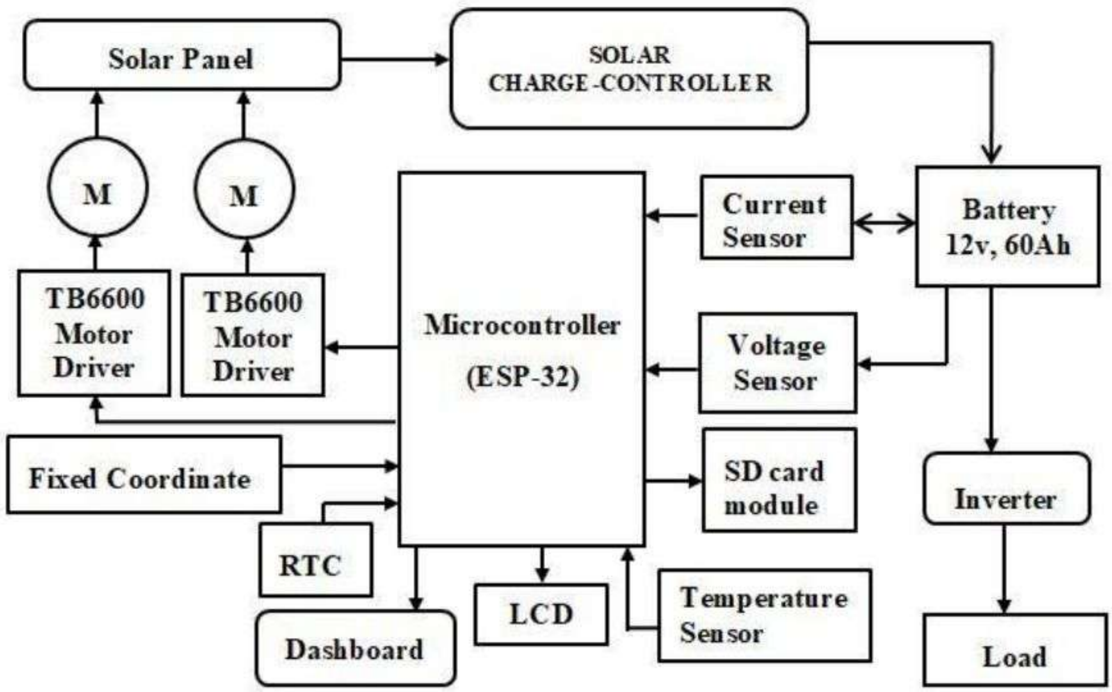

Figure 3.1 : Block Diagram Dual-Axis Solar Tracker with Inverter for Efficient Solar Energy Conversion

The block diagram illustrates the overall architecture and of the Dual-Axis Solar Tracker with Inverter for Efficient Solar Energy Conversion;

1. Solar Energy Generation and Tracking

The solar panel is mounted on **a** dual-axis mechanical structure that allows independent movement along the azimuth and elevation axes. Two NEMA 23 stepper motors are used to orient the panel toward the sun. Each motor is driven by a TB6600 motor driver**,** which receives step and direction control signals from the ESP32 microcontroller**.** Sun position is calculated using fixed geographic coordinates (determined once via a mobile-phone GPS at the installation site) and **time information from an RTC module**. Based on these inputs, the ESP32 computes the required angular position of the panel and commands the motors accordingly. This ensures continuous alignment of the panel with the sun for improved energy capture throughout the day.

2. Charge Control and Battery Storage

The DC output from the solar panel is fed into a solar charge controller, which regulates the charging process and safely charges a battery 12V, 60Ah. The charge controller protects the battery from over-charging and reverse current flow, ensuring reliable and safe energy storage.

3. Power Conversion

The stored DC power from the battery is supplied to a stand-alone inverter, which converts DC power into AC power suitable for supplying the connected load**.** The inverter operates independently without any grid connection or hybrid switching logic.

4. Monitoring and Analysis

A voltage sensor and a current sensor continuously measure the system's electrical parameters. These sensor outputs are fed back to the ESP32 microcontroller for real-time monitoring and system evaluation.

Key parameters such as solar voltage, current, battery voltage, and estimated power output are processed and displayed on an LCD**.** Additionally, system data can be visualized on a dashboard for monitoring and analysis purposes.

5. Control and Display Unit

The **ESP32 microcontroller** acts as the central control unit of the system. It performs:

Sun position calculation, motor control for dual-axis tracking, sensor data acquisition, display, and dashboard communication.

3.2 Flowchart/Algorithm

3.2.1 Algorithm

A. Initialization

1. Initialize the ESP32 microcontroller.
2. Initialize all hardware components:
    - Solar tracking motors (azimuth & elevation)
    - Voltage and current sensors
    - Inverter
    - LCD
    - ESP32
3. Set motor movement limits for safe panel operation.

B. Sun Tracking Loop (Continuous Monitoring)

1. Read angular position feedback from the dual-axis motors (e.g., potentiometers or encoders).
2. Compare current panel position with pre-calculated sun angles **based on time/date/location.**
3. Rotate the panel to align perpendicular to sunlight:
    - Adjust azimuth (horizontal rotation)
    - Adjust elevation (vertical tilt)
4. Repeat continuously to follow the sun throughout the day.

C. Power Conversion

1. Solar panel generates DC power.
2. DC power is sent to the inverter.
3. Inverter converts DC → AC for the load.
4. Monitor panel voltage and current; display on LCD/Serial Monitor.

D. Safety Protection

1. Monitor for over-voltage, over-current, and over-temperature.
2. If any fault occurs:
    - Stop motor movement

- Disconnect the inverter
- Display warning on LCD

E. Logging and Display

1. Show real-time parameters: solar voltage, current, panel angles.
2. Send data to dashboard for monitoring and analysis.

3.2.2 Flowchart

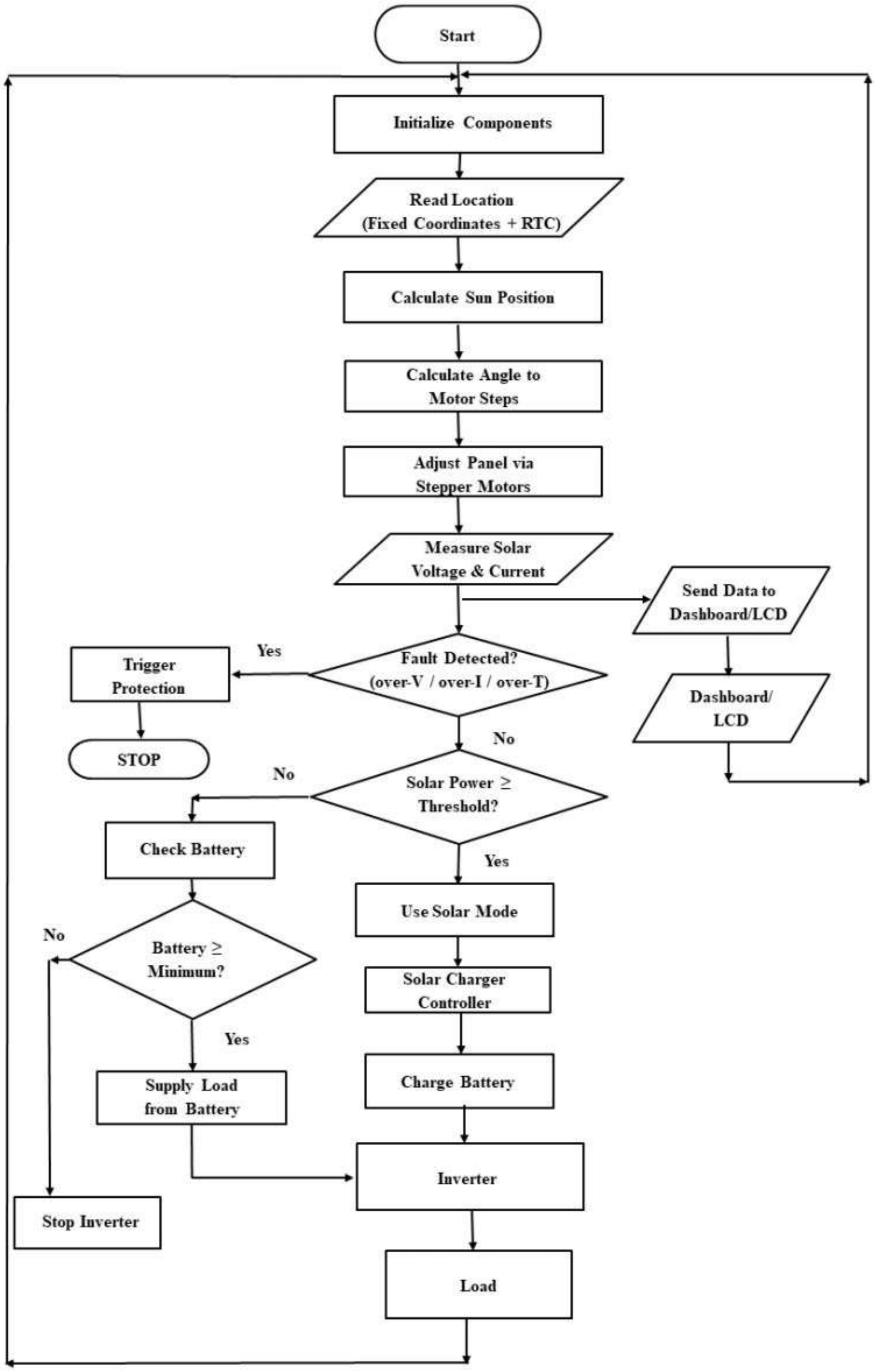

Figure 3.2 : Flowchart of Dual-Axis Solar Tracker with Inverter for Efficient Solar Energy Conversion

3.3 Solar Position Calculation (Azimuth and Elevation Angle)

To achieve accurate sensorless tracking, the position of the sun is calculated mathematically using astronomical equations based on time and geographical location as follows [23];

Input Parameters

- Latitude (φ) = 27.67° N (Bhaktapur)
- Longitude = 85.43° E
- Day number of year (n)
- Local time (from RTC)

1. Solar Declination Angle (δ)

The declination angle varies throughout the year and is calculated as:

$\delta = 23.45^\circ \sin[(360/365)(284 + n)]$

Where: δ = Solar declination angle (degrees), n = Day number of the year [24]

2. Hour Angle (H)

The hour angle represents the angular displacement of the sun from solar noon.

$H = 15^\circ (T_{solar} - 12)$

Where: Tsolar = Solar time in hours

Once T_{solar} is isolated, the Hour Angle is calculated.

3. Solar Elevation Angle (α)

The elevation angle determines how high the sun appears in the sky.

$\sin\alpha = \sin\varphi \sin\delta + \cos\varphi \cos\delta \cos H$

The calculated elevation angle determines the vertical tilt of the solar panel.

4. Solar Azimuth Angle (A)

The azimuth angle determines the horizontal direction of the sun.

$\cos A = (\sin\delta - \sin\alpha \sin\varphi) / (\cos\alpha \cos\varphi)$

The calculated azimuth angle determines the horizontal rotation of the panel.

5. Motor Step Conversion

Each NEMA 23 stepper motor has a step angle of 1.8°.

Motor Steps = Required Angle / 1.8° × Micro stepping Factor

This conversion allows precise positioning of the panel along both axes.

3.4 Tools used

3.4.1 Hardware used and description

A. Temperature Sensor DS18B20

The DS18B20 was selected because accurate temperature monitoring is essential for battery and system safety. Lead-acid batteries and stepper motors can overheat under prolonged operation, so integrating a temperature sensor ensures protection and reliable operation of the solar tracking system.

Figure 3.3 : Temperature Sensor DS18B20

B. ESP32 Microcontroller

The **ESP32** was selected as the main controller for the dual-axis solar tracker due to its dual-core processor, high processing power, built-in Wi-Fi, and multiple I/O pins. These features allow it to control stepper motors, read sensors, execute sun-tracking algorithms, and support IoT-based monitoring simultaneously. Its multitasking capability and real-time processing make it ideal for managing the integrated solar tracking system efficiently and reliably.

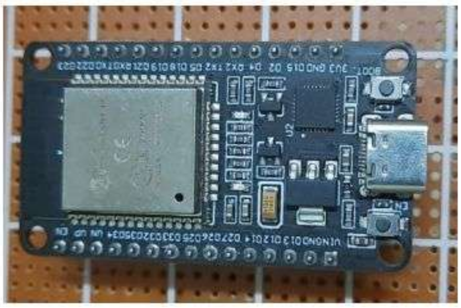

Figure 3.4 : ESP32 Microcontroller

C. Solar Panel

This panel is a 60 Wp mono-crystalline silicon solar panel, model SCM 60M, 28 manufactured by Zhejiang Shengcheng Solar Technology Co., Ltd. [21]. It consists of 36 mono-crystalline cells (125×125 mm) in series, offering higher efficiency and a compact

Figure 3.5 : Solar Panel

footprint suited to the dual-axis tracking platform. Key ratings include: Pmax 60 Wp (±5%), Voc 19.8 V, Isc 4.47 A, Vmp 17.8 V, Imp 3.38 A, max series fuse 10 A, and max system voltage 1000 V DC. It measures 910×541×30 mm, weighs 5.4 kg, and is rated for NOCT 48±2°C and operating temperature −40°C to +85°C under standard test conditions (AM1.5, 1 kW/m², 25°C). The module is CSA, TÜV, IEC, and CE certified. This panel was mounted on the tracking mechanism, with its voltage, current, and temperature output logged and compared against a static reference panel.

D. Battery

The 12 V 60Ah battery was chosen to store sufficient energy for night-time or cloudy day operation. Lead-acid batteries are cost-effective, readily available in Nepal, and reliable for small-scale solar projects. This ensures the system can provide continuous power when sunlight is insufficient.

Figure 3.6 : Lead-Acid Battery

E. Stepper Motors

The rotational actuator used is a NEMA23-size hybrid stepping motor, model SY57STH76-5004B, manufactured by Changzhou Songyang Machinery & Electronics [22]. It has a step angle of 1.8° (200 steps/revolution), a 6-wire bipolar-configurable winding, and was driven at a rated phase current as set on the TB6600 driver following coil-pair identification. The motor was selected for its high holding torque and precise step resolution, suited to slow, high-accuracy positioning required for solar tracking against wind and panel-weight loading.

Figure 3.7 : Stepper Motor

F. Stepper Motor Drivers

The TB6600 drivers were used to efficiently control the NEMA 23 motors. They support micro stepping for smooth motion, overcurrent protection, and adjustable current, which ensures accurate panel alignment and motor safety essential for consistent dual-axis tracking.

Figure 3.8 : Stepper Motor Drivers (TB6600)

G. Inverter (100watt, 220v)

The inverter in this project converts the 12 V DC output from the battery into a 220 V AC, 50 Hz supply using a center-tapped push-pull topology, making it suitable for low-power AC applications. The inverter employs two IRFZ44N N-channel MOSFETs, which are alternately switched to drive the two halves of a 12–0–12 V center-tapped transformer, generating an alternating AC voltage at the transformer secondary. The ESP32 microcontroller generates alternating SPWM signals with strict mutual exclusion using a sine lookup table to produce a near-sinusoidal output waveform with reduced harmonic distortion. An LC output filter, along with gate resistors and snubber circuits, is incorporated to suppress switching noise and improve the quality of the output waveform.

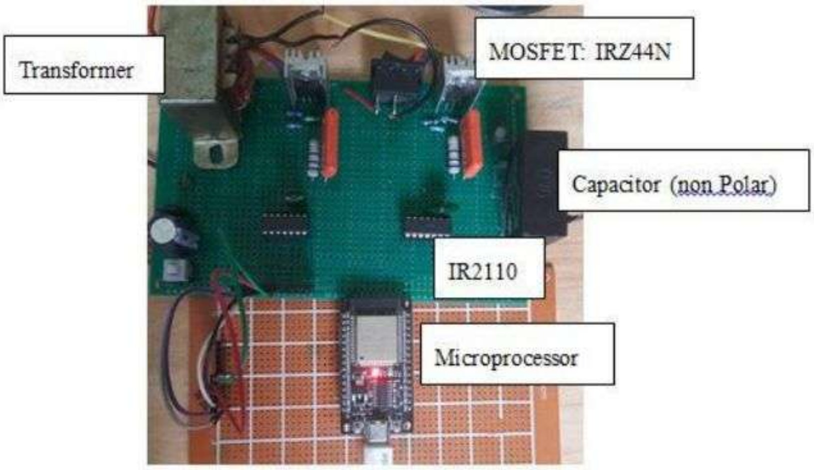

Figure 3.9 : Inverter

To ensure reliable and safe operation, the inverter incorporates overcurrent and under/over-voltage protection using an ACS712 current sensor and a battery voltage sensing circuit. The protection system continuously monitors the operating conditions and safely disconnects the inverter during abnormal conditions to prevent damage to the power electronics and connected loads. The prototype was successfully tested under various resistive loads and produced a stable 191 V AC, 50 Hz output with an overall efficiency of approximately 80–85%. The push-pull topology offers a simple, cost-effective, and efficient solution for low-voltage DC to AC power conversion, making it well suited for integration with the proposed dual-axis solar tracking system.

H. LCD Display

The 16×4 I2C LCD was selected for its compact size, low pin requirement, and ability to display real-time system data, including battery voltage, current, and power. This aligns with the project's aim of providing user-friendly monitoring and system accessibility.

Figure 3.10 : LCD Display

I. RTC Module

The RTC module provides accurate UTC time for solar position calculations, allowing the sun tracking algorithm to position the panels precisely without requiring an onboard GPS module. This supports the project's goal of efficient and sensor less dual-axis solar tracking**.**

Figure 3.11 : RTC Module

J. Micro SD-Card Module

For data backup and analysis it is used having operating voltage: 3.3V, support SPI communication and memory up to 32GB.

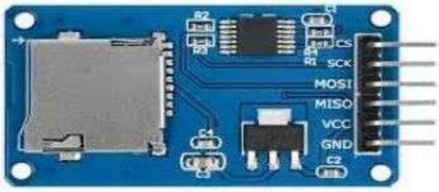

Figure 3.12 Micro - SD Card Module

K. Current Sensor

The ACS712-20A Hall-effect current sensor is used to measure the DC current flowing from the solar panel to the battery and inverter load. It operates on the Hall-effect principle, where a magnetic field generated by the current produces a proportional voltage output, providing galvanic isolation between the measured circuit and the sensing electronics. The sensor is connected in series with the battery positive line, with its OUT pin feeding an analog voltage to the ESP32 ADC on GPIO34. This allows real-time monitoring of current draw, power calculation, and overcurrent protection.

Figure 3.13 : Current Sensor

L. Voltage Sensor

A ready-made voltage sensor module is used to measure solar panel voltages. The module accepts DC input voltages from 0V to 25V and provides an analog output proportional to

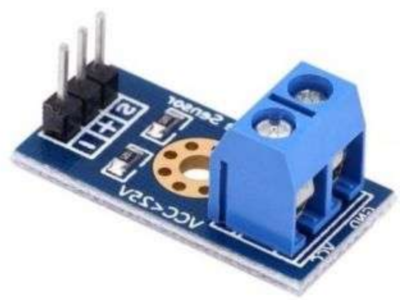

Figure 3.14 : Voltage Sensor

the measured voltage. It features a simple three-pin interface: "+" for 3.3V or 5V supply, "-" for GND, and "S" for the analog output signal to the ESP32 ADC. The input is connected via a red terminal block (VCC) and black terminal (GND). The ESP32 reads the analog value on GPIO33.

M. Solar Charge Controller

A solar charge controller is used to regulate the charging of the 12V battery from the 60W solar panel. It prevents overcharging by disconnecting the panel when the battery reaches full charge (typically 14.4V) and blocks reverse current flow from the battery to the panel at night. The controller features adjustable system voltage, built-in protection against overcharge, over-discharge, reverse polarity, and short-circuit, along with a full timer for charge management. This ensures safe battery operation, extends battery life, and maintains reliable energy storage for the inverter system.

Figure 3.15 : Solar Charge Controller

3.4.2 Software used and Description

A. PlatformIO IDE (VS Code Extension)

Primary Integrated Development Environment for writing, compiling, and uploading firmware to the ESP32.

B. ESP32 Firmware Modules

- Control dual-axis using stepper motor.
- Generate pure sine-wave using ESP32 and IR2110.

C. Proteus

This is used for circuit diagram design.

D. Vs Code Platform.IO

Programming language used in C++ for solar tracking and SPWM generation.

CHAPTER 4: RESULTS AND DISCUSSION

4.1 Completed works

4.1.1 Hardware Implementation

A. MECHANICAL DESIGN OF DUAL-AXIS SOLAR TRACKER

The mechanical structure of the dual-axis solar tracker was designed to be cost-effective, lightweight, and reliable, utilizing locally available materials suitable for Nepal's context. The primary design goal was to achieve smooth, backlash-free motion for precise panel alignment while ensuring structural stability under wind and gravitational loads.

The structure employs a modular vertical configuration where the solar panel is mounted at the top, supported by an elevation axis, which in turn rests on an azimuth axis and a stable MDF base plate. The entire framework was constructed using 3/4-inch CPVC pipes and fittings, chosen for their corrosion resistance, ease of fabrication, and widespread availability. Wooden brackets with 8mm threaded iron rods were used to secure the 60W panel, which weighs approximately 6 kg. The total moving mass, including the frame, is roughly 10 kg.

The azimuth axis (horizontal rotation) employs a single-stage timing pulley reduction of 1:3 (20T to 60T), providing smooth rotation. The elevation axis (vertical tilt), however, requires significantly higher torque to lift the panel against gravity. To achieve this without increasing motor size, a triple-stage reduction system with a total ratio of 1:36 was implemented (20T→60T, 20T→60T, and 20T→80T). This high reduction multiplies the NEMA 23 motor's torque by 36 times, providing ample force to lift the panel smoothly under wind loads and gravitational forces.

Both axes are driven by NEMA 23 (57mm frame size) stepper motors configured with 1/8 microstepping (1600 pulses per revolution). The azimuth axis achieves a tracking resolution of 0.075° per step, while the elevation axis achieves 0.00625° per step, both comfortably exceeding the 0.5° accuracy required by the Solar Position Algorithm. This high-precision mechanical design ensures accurate sun tracking throughout the day, maximizing solar energy capture for the inverter system. The ESP32 controller provides software-based limits for both axes to prevent over-travel and establish homing references. Load calculations confirmed that the 1:36 reduction provides sufficient torque for the 10 kg load, with motor temperatures remaining below 40°C during continuous operation. The high reduction ratio ensures the motor can hold the panel steady even under gusty wind conditions.

Testing confirmed smooth, vibration-free motion across the full range of both axes. The structure demonstrated stability under load, with no visible deflection or stalling during continuous operation. Motor temperatures remained within safe limits (below 40°C) after prolonged testing. The mechanical assembly successfully provides a robust, responsive platform for the solar tracker, proving that high-accuracy tracking is achievable using cost-effective, locally sourced materials and standard workshop tools. The design and implementation of the dual-axis solar tracking system were successfully completed during the mid-term phase.

All development phase of mechanical design of trackers are shown in Annex-4.

B. Inverter System (Push-Pull Technology)

This project implements a single-phase, pure sine wave push-pull 100watt inverter using an ESP32 microcontroller to convert 12V DC into 50Hz AC output. The power stage employs a center-tapped 12-0-12V transformer driven by two IRFZ44N MOSFETs through IR2110 gate drivers. Sinusoidal Pulse Width Modulation (SPWM) is implemented using a 400-point sine lookup table at a 20kHz carrier frequency, with the two MOSFETs alternately conducting on opposite halves of each output cycle. A 500ns dead time prevents shoot-through, and a soft-start ramp gradually raises the modulation index at power-up to reduce inrush current.

The firmware was developed using PlatformIO with the ESP32's hardware MCPWM peripheral generating the 20kHz carrier entirely in hardware. A dedicated timer interrupt advances the sine lookup index each carrier period, with duty cycle updates deferred to a high-priority FreeRTOS task to ensure deterministic timing. Several firmware issues were resolved during development, including unsafe ISR calls, a forced-low state fault, and a timing race condition, all verified through oscilloscope testing.

The inverter incorporates over-current protection (20A threshold via ACS712), under-voltage cutoff (10.5V), and over-temperature shutdown (85°C via NTC thermistor); with response times under 80ns through direct register manipulation. To compensate for the transformer's lower-than-ideal turns ratio (1:16 instead of the required 1:18.3), a DC-DC boost converter raises the bus voltage from 12.5V to 16V, increasing output from 148.8V RMS to 191.9V RMS at 50Hz under a 10W resistive load. No-load primary current remained stable at approximately 0.15A, confirming efficient switching operation. The inverter achieved approximately 80% efficiency under load, with losses primarily from transformer copper and core losses. An LC output filter (10mH inductor, 2.5μF capacitor, and 1kHz cutoff) attenuates the 20kHz switching component by approximately 40dB while passing the 50Hz fundamental with less than 2% attenuation.

The remaining shortfall to the 220V target is attributed to transformer winding resistance and core losses. The inverter control stage has been validated as functionally correct and stable, with further boost-stage tuning and filter integration planned to achieve the target 220V, 50Hz pure sine wave output.

Circuit diagram is shown in Annex-6.

4.1.2 Software Implementation

Firmware for both the tracking and inverter subsystems was developed in C++ using the PlatformIO IDE within Visual Studio Code, targeting the ESP32 Arduino framework.

For the tracking subsystem, the solar position algorithm described in Section 3.3 was implemented to compute the sun's real-time azimuth and elevation angles from the current date and time obtained via the RTC module and the fixed geographic coordinates of the installation site (27.67°N, 85.43°E, Bhaktapur), eliminating the need for a GPS receiver. The computed angles are converted into the corresponding number of motor steps accounting for the NEMA23 motors' 1.8° step angle and the mechanical reduction on each axis (1:3 azimuth, 1:36 elevation) and issued as step/direction pulses to the TB6600 drivers to reposition the panel.

For the inverter subsystem, the SPWM output is generated using the ESP32's hardware MCPWM peripheral driven by a pre-computed 400-point sine lookup table (LUT), producing a 20kHz switching carrier whose duty cycle traces a 50Hz sinusoidal envelope. Dead-time insertion and a soft-start ramp are implemented within the same SPWM routine to prevent shoot-through and limit inrush current at startup.

4.1.3 Web Dashboard Development

A web-based dashboard was developed using the ESP32's built-in Wi-Fi Access Point (AP) and Webserver. The interface, built with HTML, CSS, and JavaScript, displays real-time voltage, current, power, energy, and solar tracking angles, with data recorded every 3 minutes and tracking angles re-evaluated and updated every 15 minutes. It also provides manual control of the azimuth and elevation angles while allowing users to switch between automatic and manual tracking through a web browser. Figure is shown in Annex-5.

4.1.4 Data Collection Overview

Performance data for both the static panel and the dual-axis tracker were logged simultaneously on 1 July 2026 between 10:00 AM and 4:00 PM, at 3-minute intervals, yielding 121 readings per system. Voltage, current, and power were recorded directly from the panel output; for the dual-axis system, azimuth angle, elevation angle, were additionally logged to characterize the tracking behavior and conversion performance.

A. Static Panel Observations

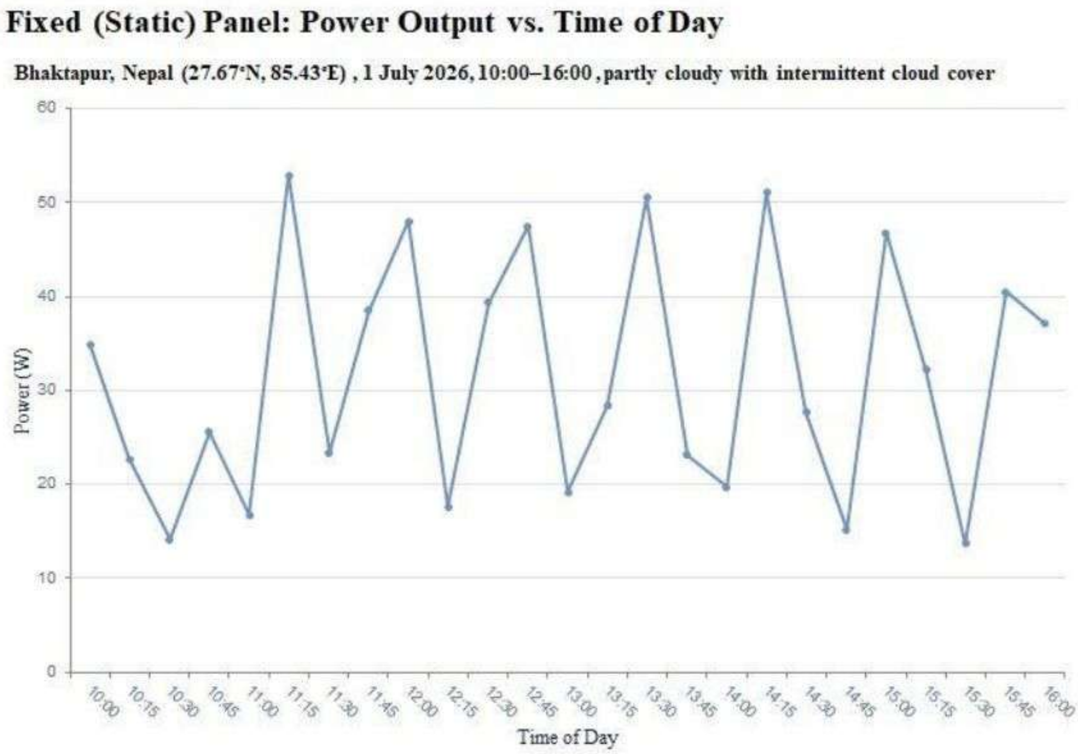

Figure 4.1: Static Panel

The fixed panel's power output was recorded at Bhaktapur, Nepal (27.67°N, 85.43°E) on 1 July 2026, between 10:00 and 16:00, under partly cloudy conditions with intermittent cloud cover which was facing south with elevation 30°. Over this session the output swung repeatedly between about 13.5 W (at 13:54) and 53.7 W (at 11:54).

Because the panel's tilt is fixed, its output is close to maximum only in the brief moments when the sun's position happens to align with the panel's fixed angle. As the sun moves away from that alignment, output falls quickly, then climbs again as the sun's path brings it back into rough alignment later in the day. This is why Figure 4.1 shows seven distinct peaks and dips over the session rather than a single smooth hump centered on solar noon. Part of this variation is shared with the tracker's data and is attributable to passing cloud cover, but the repeated saw-tooth pattern itself is a direct, expected consequence of a fixed panel losing and regaining alignment with the sun throughout the day.

B. Dual-Axis Tracker Observations

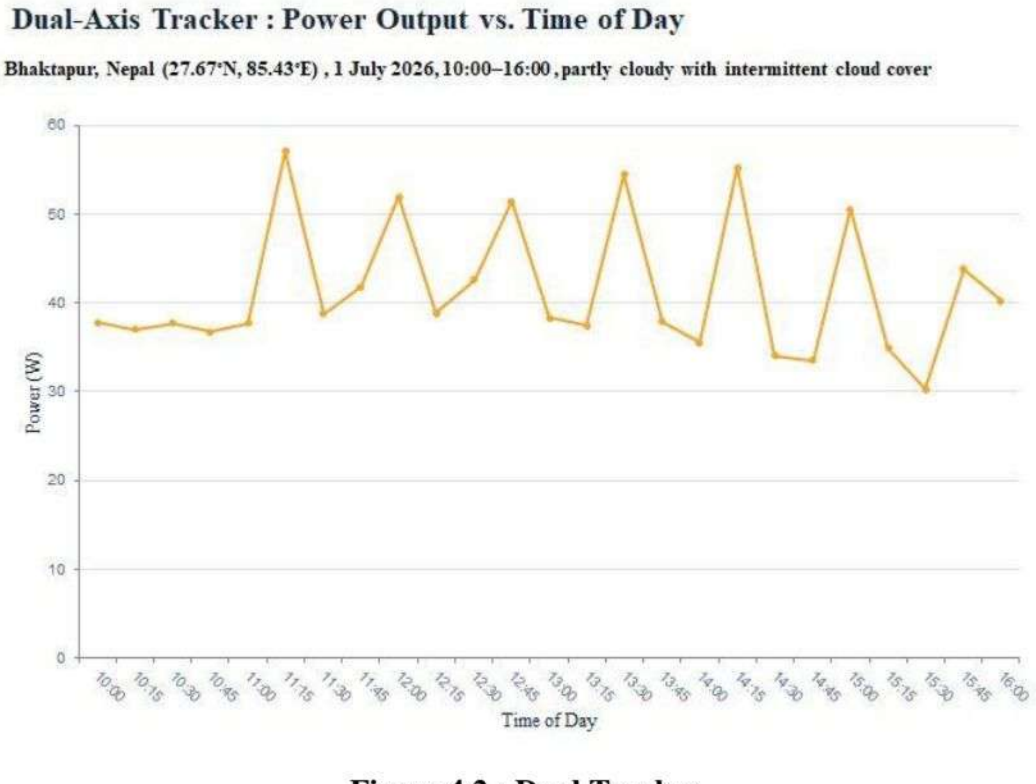

Figure 4.2 : Dual Tracker

The dual-axis tracker was tested at the same location and under the same sky conditions, simultaneously with the fixed panel. Its power stayed within a much narrower band about 28.6 W (at 15:36) to 58.0 W (at 11:54).

Over the session, the azimuth angle rotated steadily from about 92° to 279°, tracking the sun from east to west, while the sun's elevation angle rose to a peak of about 85° near solar noon (12:00), corresponding to the panel lying nearly flat to directly face the near-overhead sun. This continuous repositioning kept the panel much closer to perpendicular with the incoming sunlight throughout the day, which is why Figure 4.2 shows a curve that stays both higher and smoother than the fixed panel's. The small dips that do appear in the tracker's own curve (near 11:36 and 14:42) line up closely in time with dips in the fixed panel's curve this shared timing is the basis for inferring intermittent cloud cover during the session, rather than a tracking fault of the panel itself.

4.1.5 Comparison Analysis

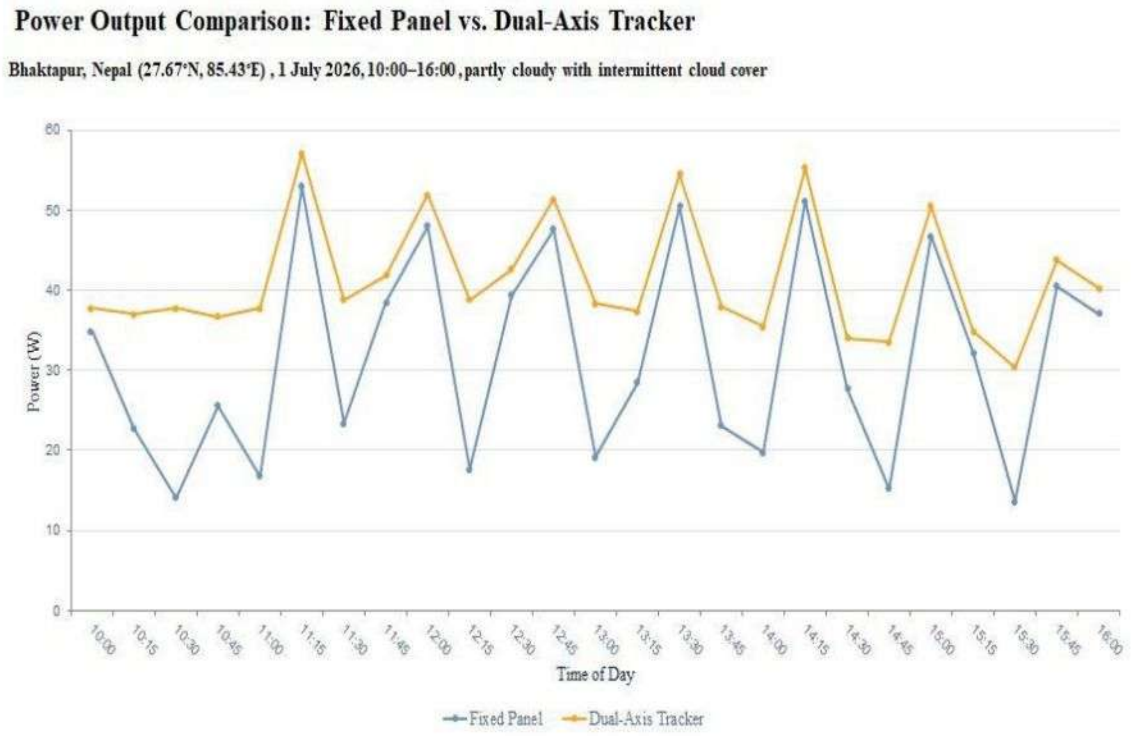

Figure 4.3 : Power output Comparison

Both the static panel and the dual-axis tracker were tested simultaneously under identical environmental conditions from 10:00 AM to 4:00 PM, with performance data recorded every 3 minutes to ensure a fair comparison. The dual-axis tracker achieved a 32.0% higher average power output (41.3 W vs. 31.3 W).

The tracker's continuous repositioning keeps it closer to normal incidence throughout the session, which is why its curve stays both higher and smoother than the fixed panels even under the same intermittent cloud cover.

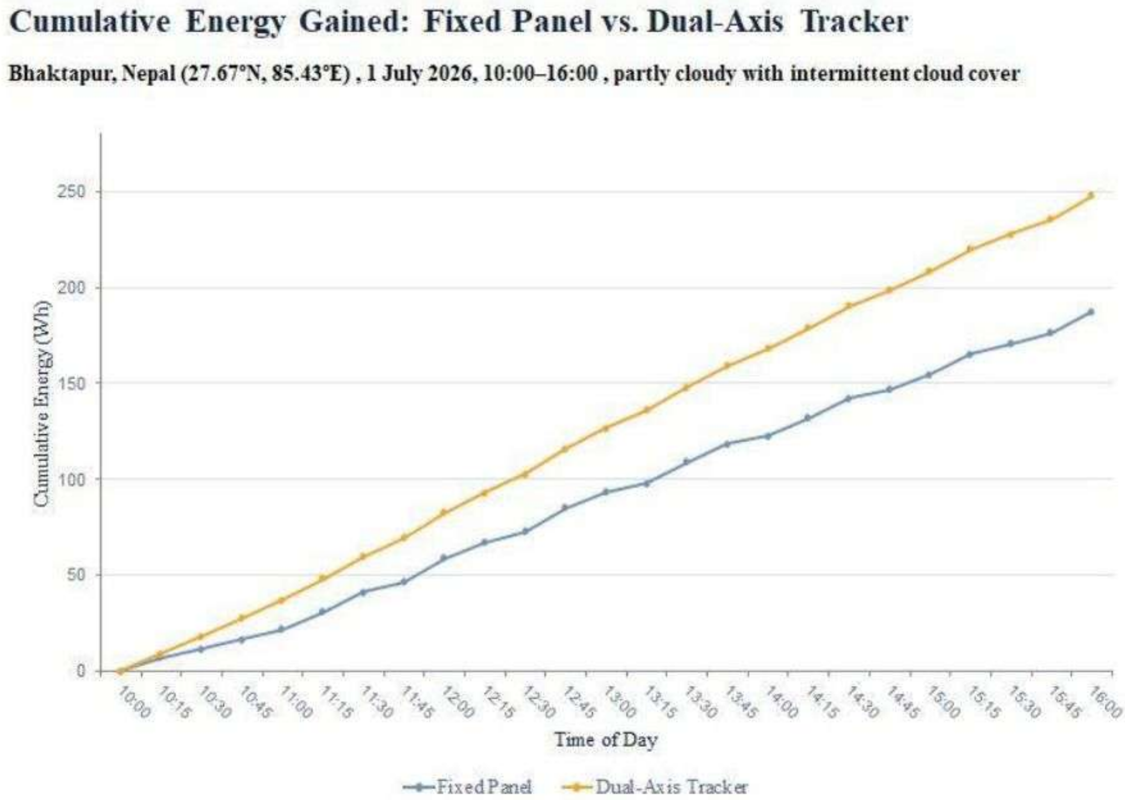

Figure 4.4 : Cumulative energy gained: Fixed panel vs. Dual-axis tracker

Figure 4.4 shows the running total of energy delivered by each system over the test session at Bhaktapur, Nepal (27.67°N, 85.43°E) on 1 July 2026, from 10:00 to 16:00, under the partly cloudy conditions.

Over the six-hour session, the fixed panel delivered a total of 187.48 Wh, while the dual-axis tracker delivered 247.83 Wh, 32.2% improvement, consistent with the independently measured 32.0% average power gain. The tracker's curve climbs more steeply and stays consistently above the fixed panels throughout the session, reflecting the higher, smoother power output. Because the test window is a six-hour, midday-biased session rather than a full sunrise-to-sunset day, this figure understates the tracker's advantage under real full-day operation: a fixed panel is already close to normal incidence around solar noon, and loses the most ground in the early morning and late afternoon hours, which this session only partially covers.

CHAPTER 5: CONCLUSION AND FUTURE ENHANCEMENT

5.1 Conclusion

This project successfully achieved its primary objective of designing and implementing a Dual-Axis Solar Tracker with an Inverter for Efficient Solar Energy Conversion. The work encompassed the complete design, fabrication, integration, and performance evaluation of an intelligent photovoltaic system capable of maximizing solar energy harvesting while providing usable AC power and real-time monitoring.

The dual-axis solar tracking mechanism was successfully designed and fabricated using CPVC pipes, timing pulleys, belts, and high-torque stepper motors, providing smooth movement along both azimuth and elevation axes. The intelligent control system was developed using an ESP32 microcontroller programmed with a solar position algorithm to automatically track the sun throughout the day, with manual override capability for user flexibility. The push-pull inverter successfully converted 12V DC power into 50Hz AC output, reaching approximately 192V RMS against a 220V design target, making the harvested solar energy suitable for conventional AC loads. A real-time monitoring and control system was developed using the ESP32's built-in Wi-Fi, displaying voltage, current, power, energy, battery status, and tracking angles on a web dashboard with data logged every 3 minutes and panel angles re-evaluated every 15 minutes, along with remote manual control capability.

Comprehensive experimental testing was conducted by operating the dual-axis tracker and a fixed solar panel simultaneously under identical conditions from 10:00 AM to 4:00 PM with measurements recorded every three minutes. The dual-axis tracker achieved approximately 32.0% higher average power output, 32.2% greater total energy yield over the six-hour test session. The system maintained consistent power generation throughout the day by continuously adjusting panel orientation.

In conclusion, the proposed system successfully demonstrates that intelligent dual-axis tracking significantly enhances photovoltaic energy harvesting compared to conventional fixed systems while providing stable AC power through the integrated push-pull inverter. The developed prototype represents a practical, reliable, and cost-effective renewable energy solution suitable for standalone applications, contributing to more efficient utilization of solar resources.

5.2 Future Enhancements

While the developed system meets its intended objectives, the following enhancements are identified for future development:

Long-term performance evaluation: Extended testing across seasons and varying weather conditions to validate consistency, durability, and long-term energy gains.

Battery monitoring and energy management: State-of-charge estimation with intelligent charge/discharge control for improved energy utilization and battery protection.

Cloud-based remote monitoring: Extending the local Wi-Fi dashboard with cloud connectivity for remote access, historical data storage, and performance analysis from any location.

Weather protection: Integration of wind and rainfall sensors to automatically stop the panel during adverse conditions, improving mechanical durability.

Mobile application support: A companion mobile app for real-time notifications and simplified remote monitoring alongside the web dashboard.

MPPT implementation: Integration of Maximum Power Point Tracking for optimized solar energy harvesting.

Grid-tied capability: Extension for grid-connected operation allowing excess energy export.

REFERENCES

[1] H. Mousazadeh, A. Keyhani, A. Javadi, H. Mobil, K. Abrinia, and A. Sharifi, "A review of principle and sun-tracking methods for maximizing solar systems output," *Renew. Sustain. Energy Rev.*, vol. 13, no. 8, pp. 1800–1818, Oct. 2009.

[2] K. K. Chong and C. W. Wong, "General formula for on-axis sun-tracking system and its application in improving tracking accuracy of solar collector," *Sol. Energy*, vol. 83, no. 3, pp. 298–305, Mar. 2009.

[3] I. Reda and A. Andreas, "Solar position algorithm for solar radiation applications," *Sol. Energy*, vol. 76, no. 5, pp. 577–589, May 2004.

[4] F. González-Longatt, P. R. R. d. S. Junior, and J. L. R. Torres, "A simple solar position algorithm for control systems," *IEEE Latin Amer. Trans.*, vol. 10, no. 2, pp. 1653–1657, Mar. 2012.

[5] Y. Chen and K. M. Smedley, "A cost-effective single-stage inverter with maximum power point tracking," *IEEE Trans. Power Electron.*, vol. 19, no. 5, pp. 1289–1294, Sep. 2004.

[6] *IEEE Standard for Interconnection and Interoperability of Distributed Energy Resources with Associated Electric Power Systems Interfaces*, IEEE Standard 1547-2018, 2018.

[7] *Safety of Power Converters for Use in Photovoltaic Power Systems—Part 1: General Requirements*, IEC Standard 62109-1, 2010.

[8] B. Singh, S. Singh, A. Chandra, and K. Al-Haddad, "Comprehensive study of single-phase AC-DC power factor corrected converters with high-frequency isolation," *IEEE Trans. Ind. Informat.*, vol. 7, no. 4, pp. 540–556, Nov. 2011.

[9] K. T. Lee, S. K. Lee, and J. H. Lee, "IoT-based solar monitoring system using ESP32 microcontroller," *J. Phys., Conf. Ser.*, vol. 1432, no. 1, p. 012065, Jan. 2020.

[10] M. B. Prakash and K. Govindarajulu, "Analysis and testing of dual-axis solar tracker for standalone PV systems using worm gear," *International Journal for Modern Trends in Science and Technology*, vol. 8, no. 01, pp. 1–8, Jan. 2022, doi: 10.46501/IJMTST0801001

[11] Taha, M. T., Mohamed, E. O., Abdulsalam, A. M., & Taha, A. B. (2021, February). Control of Single-Axis and Dual-Axis Solar Tracking System. In 2020 International

Conference on Computer, Control, Electrical, and Electronics Engineering (ICCCEEE) (pp. 1-6). IEEE.

[12]. Dileep D. K. and Bharath K. R., "A brief study of solar home inverters," in *Proceedings of the 2018 International Conference on Control, Power, Communication and Computing Technologies (ICCPCCT)*, Kannur, India, 2018, pp. 334–339.

[13]. Biju K. and Ramchand R., "Control of a novel single-phase grid-connected solar PV/battery hybrid energy system," in *Proceedings of the 10th Asian Control Conference (ASCC)*, Kota Kinabalu, Malaysia, 2015, pp. 1–4, doi: 10.1109/ASCC.2015.7244436

[14] M. A. Vega-Durán, J. E. Solano, and L. G. Gutiérrez, "Design and implementation of a custom PCB for embedded solar tracking control systems," *Int. J. Renew. Energy Res.*, vol. 11, no. 2, pp. 678–686, 2021.

[15] A. Gupta, P. Sharma, and V. Kumar, "ESP32-based custom PCB design for IoT-enabled sensor fusion in solar energy applications," in *Proc. IEEE Int. Conf. Renewable Energy and Smart Grid*, 2022, pp. 112–117.

[16] D. K. Nayak and R. Krishnamurthy, "Cloud-based visualization and automated fault detection for remote solar energy monitoring systems," *Energy Reports*, vol. 8, pp. 3210–3221, 2022.

[17] S. Abdallah and S. Nijmeh, "Two axes sun tracking system with PLC control," *Energy Convers. Manage,* vol. 45, no. 11–12, pp. 1931–1939, 2004.

[18] K. Suresh and M. Venugopal, "Power management optimization techniques for ESP32-based embedded solar systems," in *Proc. 2nd Int. Conf. Emerging Trends in Engineering and Technology*, 2023, pp. 201–207.

[19] M. R. Islam, K. Kamarudin, and M. A. Matin, "Experimental performance evaluation of fixed versus dual-axis tracked photovoltaic panels under field conditions," *Renewable Energy*, vol. 78, pp. 576–585, Jun. 2015.

[20] S. Seme, G. Stumberger, and J. Vorsic, "Maximum efficiency trajectories of a two-axis sun tracking system determined considering tracking system consumption," *IEEE Trans. Power Electron.*, vol. 26, no. 4, pp. 1280–1290, Apr. 2011.

[21] Zhejiang Shengcheng Solar Technology Co., Ltd., *Smart Solar Module SCM 60M – Product Datasheet*, 2020.

[22] Changzhou Songyang Machinery & Electronics Co., Ltd., *SY57STH76 Series Hybrid Stepping Motor Datasheet*.

[23] J. A. Duffie and W. A. Beckman, Solar Engineering of Thermal Processes, 4th ed. Hoboken, NJ: John Wiley & Sons, 2013.

[24] p. I. Cooper, "The absorption of solar radiation in solar stills, “Solar energy, vol. 12, no. 3, pp. 333–346, 1969.

GANTT CHART

Task	Week 1-2	Week 3-4	Week 5-6	Week 7-8	Week 9-10	Week 11-12	Week 13-14	Week 15-16
1.Planning & Research	■	■						
2.Component Selection & Procurement	■	■	■					
3. Hardware Assembly (Mechanical)		■	■	■				
4. Firmware Development (ESP32)			■	■	■			
5. Fixed-Coordinate Sun Tracking Algorithm				■	■			
6. Motor Control & Sensor Integration				■	■	■		
7. Testing & Calibration					■	■		
8. Data collection and Analysis						■	■	
9. Inverter Circuit Design (100W)						■	■	
10. Final System Integration								■
11. Documentation & Report Writing	■	■	■	■	■	■	■	■

ANNEX-1

Cost Incurred

Solar panel 60 Watt	3000	Provided by college
Battery 60 Ah, 12v	13000	Provided by college

Dual tracker with inverter

S.N.	COMPONENTS	COST	Remarks
1.	Microcontroller(ESP32)	800	
2.	Temperature Sensor	150	
3.	Transformer(12-0-12,220v,1Amp)	650	
5.	LCD Display (16x4 I2C)	800	
6.	Stepper motor Nema 23 (2)	8000	Provided by college
7.	Motor driver (2)	2400	Provided by college
8.	Bearing (9), Bush (10 to 8mm)	2300	
9.	CPVC (Tee, Elbow, pipe, joint)	4400	
10.	Miscellaneous (switch, wires.)	1300	
11.	Pulley (80T,60T,20T), Belt(2m)	3400	
12.	SD card Module	300	
13.	DC Fuse 15A (1)	15	
14.	Capacitors	155	
15.	Driver IC IR2110(2)	125	
16.	MOSFET IRFZ44N(2)	180	
17.	Resistors 45k,10k,4.7k (4)	100	
18.	Inductor 33mH	60	
19.	Current and voltage Sensor	350	
20.	RTC Module	250	
Total		**Rs 25,735**	

ANNEX-2

Static Panel Data: Facing South with Elevation angle 30°

Entry	Timestamp	Voltage (V)	Current (A)	Power(W) = Voltage × Current	Cumulative Energy (Wh)
1	7/1/2026 10:00	13.72	2.54	34.85	0.00
2	7/1/2026 10:03	13.66	2.32	31.69	1.66
3	7/1/2026 10:06	13.62	2.15	29.28	3.19
4	7/1/2026 10:09	13.58	1.94	26.35	4.58
5	7/1/2026 10:12	13.55	1.82	24.66	5.85
6	7/1/2026 10:15	13.52	1.68	22.71	7.04
7	7/1/2026 10:18	13.48	1.51	20.35	8.11
8	7/1/2026 10:21	13.46	1.38	18.57	9.09
9	7/1/2026 10:24	13.42	1.22	16.37	9.96
10	7/1/2026 10:27	13.40	1.11	14.87	10.74
11	7/1/2026 10:30	13.38	1.05	14.05	11.47
12	7/1/2026 10:33	13.41	1.21	16.23	12.22
13	7/1/2026 10:36	13.45	1.38	18.56	13.09
14	7/1/2026 10:39	13.50	1.54	20.79	14.08
15	7/1/2026 10:42	13.55	1.72	23.31	15.18
16	7/1/2026 10:45	13.59	1.88	25.55	16.40
17	7/1/2026 10:48	13.61	1.95	26.54	17.70
18	7/1/2026 10:51	13.56	1.74	23.59	18.96
19	7/1/2026 10:54	13.49	1.42	19.16	20.02
20	7/1/2026 10:57	13.44	1.15	15.46	20.89
21	7/1/2026 11:00	13.42	1.25	16.78	21.70
22	7/1/2026 11:03	13.40	1.88	25.19	22.74
23	7/1/2026 11:06	13.45	2.45	32.95	24.20
24	7/1/2026 11:09	13.51	3.12	42.15	26.08
25	7/1/2026 11:12	13.58	3.65	49.57	28.37
26	7/1/2026 11:15	13.62	3.88	52.85	30.93
27	7/1/2026 11:18	13.59	3.71	50.42	33.51
28	7/1/2026 11:21	13.55	3.42	46.34	35.93
29	7/1/2026 11:24	13.48	2.95	39.77	38.08
30	7/1/2026 11:27	13.42	2.38	31.94	39.88
31	7/1/2026 11:30	13.39	1.75	23.43	41.26
32	7/1/2026 11:33	13.35	1.22	16.29	42.25
33	7/1/2026 11:36	13.38	1.08	14.45	43.02
34	7/1/2026 11:39	13.41	1.45	19.44	43.87
35	7/1/2026 11:42	13.46	2.12	28.54	45.07
36	7/1/2026 11:45	13.52	2.85	38.53	46.74

37	7/1/2026 11:48	13.55	3.34	45.26	48.84
38	7/1/2026 11:51	13.58	3.72	50.52	51.23
39	7/1/2026 11:54	13.60	3.95	53.72	53.84
40	7/1/2026 11:57	13.57	3.81	51.70	56.47
41	7/1/2026 12:00	13.53	3.55	48.03	58.97
42	7/1/2026 12:03	13.49	3.15	42.49	61.23
43	7/1/2026 12:06	13.44	2.68	36.02	63.19
44	7/1/2026 12:09	13.40	2.15	28.81	64.81
45	7/1/2026 12:12	13.37	1.68	22.46	66.10
46	7/1/2026 12:15	13.34	1.32	17.61	67.10
47	7/1/2026 12:18	13.32	1.11	14.79	67.91
48	7/1/2026 12:21	13.35	1.25	16.69	68.70
49	7/1/2026 12:24	13.39	1.62	21.69	69.65
50	7/1/2026 12:27	13.43	2.25	30.22	70.95
51	7/1/2026 12:30	13.48	2.92	39.36	72.69
52	7/1/2026 12:33	13.52	3.48	47.05	74.85
53	7/1/2026 12:36	13.55	3.75	50.81	77.30
54	7/1/2026 12:39	13.58	3.91	53.10	79.90
55	7/1/2026 12:42	13.54	3.82	51.72	82.52
56	7/1/2026 12:45	13.50	3.52	47.52	85.00
57	7/1/2026 12:48	13.45	3.18	42.77	87.26
58	7/1/2026 12:51	13.41	2.72	36.48	89.24
59	7/1/2026 12:54	13.38	2.24	29.97	90.90
60	7/1/2026 12:57	13.34	1.81	24.15	92.25
61	7/1/2026 13:00	13.31	1.44	19.17	93.33
62	7/1/2026 13:03	13.29	1.18	15.68	94.20
63	7/1/2026 13:06	13.27	1.04	13.80	94.94
64	7/1/2026 13:09	13.30	1.22	16.23	95.69
65	7/1/2026 13:12	13.34	1.55	20.68	96.61
66	7/1/2026 13:15	13.38	2.12	28.37	97.84
67	7/1/2026 13:18	13.43	2.78	37.34	99.48
68	7/1/2026 13:21	13.47	3.31	44.59	101.53
69	7/1/2026 13:24	13.51	3.68	49.72	103.89
70	7/1/2026 13:27	13.54	3.85	52.13	106.44
71	7/1/2026 13:30	13.50	3.74	50.49	109.00
72	7/1/2026 13:33	13.46	3.45	46.44	111.42
73	7/1/2026 13:36	13.41	3.08	41.30	113.62
74	7/1/2026 13:39	13.37	2.62	35.03	115.53
75	7/1/2026 13:42	13.33	2.15	28.66	117.12
76	7/1/2026 13:45	13.30	1.74	23.14	118.41
77	7/1/2026 13:48	13.27	1.38	18.31	119.45
78	7/1/2026 13:51	13.25	1.14	15.11	120.28
79	7/1/2026 13:54	13.24	1.02	13.50	121.00

80	7/1/2026 13:57	13.26	1.18	15.65	121.73
81	7/1/2026 14:00	13.30	1.48	19.68	122.61
82	7/1/2026 14:03	13.34	2.02	26.95	123.78
83	7/1/2026 14:06	13.39	2.65	35.48	125.34
84	7/1/2026 14:09	13.44	3.22	43.28	127.31
85	7/1/2026 14:12	13.48	3.58	48.26	129.60
86	7/1/2026 14:15	13.51	3.78	51.07	132.08
87	7/1/2026 14:18	13.47	3.65	49.17	134.58
88	7/1/2026 14:21	13.43	3.38	45.39	136.95
89	7/1/2026 14:24	13.38	2.98	39.87	139.08
90	7/1/2026 14:27	13.34	2.52	33.62	140.92
91	7/1/2026 14:30	13.30	2.08	27.66	142.45
92	7/1/2026 14:33	13.27	1.65	21.90	143.69
93	7/1/2026 14:36	13.24	1.31	17.34	144.67
94	7/1/2026 14:39	13.22	1.10	14.54	145.47
95	7/1/2026 14:42	13.21	1.03	13.61	146.17
96	7/1/2026 14:45	13.23	1.15	15.21	146.89
97	7/1/2026 14:48	13.27	1.42	18.84	147.74
98	7/1/2026 14:51	13.31	1.92	25.56	148.85
99	7/1/2026 14:54	13.36	2.54	33.93	150.34
100	7/1/2026 14:57	13.41	3.12	41.84	152.23
101	7/1/2026 15:00	13.45	3.48	46.81	154.45
102	7/1/2026 15:03	13.48	3.72	50.15	156.87
103	7/1/2026 15:06	13.44	3.58	48.12	159.33
104	7/1/2026 15:09	13.40	3.28	43.95	161.63
105	7/1/2026 15:12	13.35	2.88	38.45	163.69
106	7/1/2026 15:15	13.31	2.42	32.21	165.46
107	7/1/2026 15:18	13.27	1.98	26.27	166.92
108	7/1/2026 15:21	13.24	1.58	20.92	168.10
109	7/1/2026 15:24	13.22	1.26	16.66	169.04
110	7/1/2026 15:27	13.20	1.08	14.26	169.81
111	7/1/2026 15:30	13.19	1.04	13.72	170.51
112	7/1/2026 15:33	13.22	1.14	15.07	171.23
113	7/1/2026 15:36	13.26	1.38	18.30	172.07
114	7/1/2026 15:39	13.30	1.82	24.21	173.13
115	7/1/2026 15:42	13.35	2.42	32.31	174.54
116	7/1/2026 15:45	13.40	3.02	40.47	176.36
117	7/1/2026 15:48	13.44	3.38	45.43	178.51
118	7/1/2026 15:51	13.47	3.62	48.76	180.86
119	7/1/2026 15:54	13.43	3.48	46.74	183.25
120	7/1/2026 15:57	13.39	3.18	42.58	185.48
121	7/1/2026 16:00	13.34	2.78	37.09	187.48

Dual Axis Solar Tracker Data

Entry	Timestamp	Azimuth (deg)	Elevation (deg)	Voltage (V)	Current (A)	Power (W) =Voltage × Current	Cumulative Energy (Wh)
1	7/1/2026 10:00	92.07	60.89	14.52	2.60	37.75	0.00
2	7/1/2026 10:03	92.49	61.55	14.57	2.46	35.84	1.84
3	7/1/2026 10:06	92.91	62.22	14.56	2.48	36.11	3.64
4	7/1/2026 10:09	93.32	62.88	14.60	2.48	36.21	5.45
5	7/1/2026 10:12	93.74	63.55	14.57	2.46	35.84	7.25
6	7/1/2026 10:15	94.16	64.21	14.51	2.55	37.00	9.07
7	7/1/2026 10:18	94.65	64.87	14.56	2.51	36.55	10.91
8	7/1/2026 10:21	95.14	65.53	14.53	2.54	36.91	12.74
9	7/1/2026 10:24	95.62	66.19	14.56	2.57	37.42	14.60
10	7/1/2026 10:27	96.11	66.85	14.62	2.56	37.43	16.47
11	7/1/2026 10:30	96.60	67.51	14.60	2.58	37.67	18.35
12	7/1/2026 10:33	97.19	68.17	14.56	2.56	37.27	20.22
13	7/1/2026 10:36	97.79	68.83	14.56	2.55	37.13	22.08
14	7/1/2026 10:39	98.38	69.48	14.60	2.57	37.52	23.95
15	7/1/2026 10:42	98.98	70.14	14.56	2.50	36.40	25.80
16	7/1/2026 10:45	99.57	70.80	14.58	2.52	36.74	27.63
17	7/1/2026 10:48	100.34	71.45	14.62	2.52	36.84	29.47
18	7/1/2026 10:51	101.11	72.10	14.64	2.54	37.19	31.32
19	7/1/2026 10:54	101.87	72.75	14.63	2.61	38.18	33.20
20	7/1/2026 10:57	102.64	73.40	14.55	2.57	37.39	35.09
21	7/1/2026 11:00	103.41	74.05	14.63	2.58	37.75	36.97

22	7/1/2026 11:03	104.48	74.69	14.62	2.67	39.04	38.89
23	7/1/2026 11:06	105.55	75.33	14.64	2.59	37.92	40.81
24	7/1/2026 11:09	106.61	75.96	14.68	3.11	45.65	42.90
25	7/1/2026 11:12	107.68	76.60	14.57	3.68	53.62	45.38
26	7/1/2026 11:15	108.75	77.24	14.61	3.91	57.13	48.15
27	7/1/2026 11:18	110.40	77.85	14.65	3.72	54.50	50.94
28	7/1/2026 11:21	112.05	78.47	14.59	3.43	50.04	53.56
29	7/1/2026 11:24	113.70	79.08	14.68	2.93	43.01	55.88
30	7/1/2026 11:27	115.35	79.70	14.65	2.54	37.21	57.89
31	7/1/2026 11:30	117.00	80.31	14.67	2.64	38.73	59.79
32	7/1/2026 11:33	119.91	80.86	14.63	2.64	38.62	61.72
33	7/1/2026 11:36	122.83	81.41	14.67	2.60	38.14	63.64
34	7/1/2026 11:39	125.74	81.97	14.68	2.56	37.58	65.53
35	7/1/2026 11:42	128.66	82.52	14.65	2.64	38.68	67.44
36	7/1/2026 11:45	131.57	83.07	14.66	2.85	41.78	69.45
37	7/1/2026 11:48	137.21	83.45	14.66	3.34	48.96	71.72
38	7/1/2026 11:51	142.85	83.84	14.62	3.73	54.53	74.31
39	7/1/2026 11:54	148.48	84.22	14.65	3.96	58.01	77.12
40	7/1/2026 11:57	154.12	84.61	14.65	3.81	55.82	79.97
41	7/1/2026 12:00	159.76	84.99	14.66	3.54	51.90	82.66
42	7/1/2026 12:03	167.83	84.99	14.68	3.13	45.95	85.11
43	7/1/2026 12:06	175.90	84.99	14.62	2.67	39.04	87.23
44	7/1/2026 12:09	183.97	84.99	14.65	2.70	39.56	89.19
45	7/1/2026 12:12	192.04	84.99	14.69	2.67	39.22	91.16

46	7/1/2026 12:15	200.11	84.99	14.63	2.65	38.77	93.11
47	7/1/2026 12:18	205.76	84.61	14.62	2.71	39.62	95.07
48	7/1/2026 12:21	211.40	84.22	14.65	2.58	37.80	97.01
49	7/1/2026 12:24	217.05	83.84	14.67	2.60	38.14	98.91
50	7/1/2026 12:27	222.69	83.45	14.64	2.59	37.92	100.81
51	7/1/2026 12:30	228.34	83.07	14.68	2.90	42.57	102.82
52	7/1/2026 12:33	231.26	82.52	14.67	3.47	50.90	105.16
53	7/1/2026 12:36	234.18	81.97	14.66	3.74	54.83	107.80
54	7/1/2026 12:39	237.10	81.41	14.65	3.91	57.28	110.60
55	7/1/2026 12:42	240.02	80.86	14.70	3.80	55.86	113.43
56	7/1/2026 12:45	242.94	80.31	14.63	3.51	51.35	116.11
57	7/1/2026 12:48	244.59	79.70	14.57	3.18	46.33	118.56
58	7/1/2026 12:51	246.25	79.09	14.68	2.69	39.49	120.70
59	7/1/2026 12:54	247.90	78.47	14.61	2.70	39.45	122.67
60	7/1/2026 12:57	249.56	77.86	14.63	2.74	40.09	124.66
61	7/1/2026 13:00	251.21	77.25	14.66	2.61	38.26	126.62
62	7/1/2026 13:03	252.28	76.61	14.57	2.56	37.30	128.51
63	7/1/2026 13:06	253.35	75.97	14.58	2.50	36.45	130.35
64	7/1/2026 13:09	254.41	75.34	14.56	2.61	38.00	132.22
65	7/1/2026 13:12	255.48	74.70	14.58	2.55	37.18	134.09
66	7/1/2026 13:15	256.55	74.06	14.62	2.56	37.43	135.96
67	7/1/2026 13:18	257.32	73.41	14.61	2.77	40.47	137.91
68	7/1/2026 13:21	258.09	72.76	14.60	3.30	48.18	140.12
69	7/1/2026 13:24	258.85	72.11	14.55	3.69	53.69	142.67

70	7/1/2026 13:27	259.62	71.46	14.52	3.88	56.34	145.42
71	7/1/2026 13:30	260.39	70.81	14.58	3.74	54.53	148.19
72	7/1/2026 13:33	260.98	70.15	14.56	3.45	50.23	150.81
73	7/1/2026 13:36	261.58	69.49	14.59	3.06	44.65	153.18
74	7/1/2026 13:39	262.17	68.84	14.59	2.60	37.93	155.25
75	7/1/2026 13:42	262.77	68.18	14.57	2.53	36.86	157.12
76	7/1/2026 13:45	263.36	67.52	14.58	2.60	37.91	158.99
77	7/1/2026 13:48	263.85	66.86	14.56	2.52	36.69	160.85
78	7/1/2026 13:51	264.34	66.20	14.56	2.55	37.13	162.70
79	7/1/2026 13:54	264.82	65.53	14.52	2.48	36.01	164.53
80	7/1/2026 13:57	265.31	64.87	14.53	2.44	35.45	166.31
81	7/1/2026 14:00	265.80	64.21	14.54	2.44	35.48	168.09
82	7/1/2026 14:03	266.22	63.55	14.55	2.44	35.50	169.86
83	7/1/2026 14:06	266.64	62.89	14.51	2.65	38.45	171.71
84	7/1/2026 14:09	267.05	62.22	14.53	3.22	46.79	173.84
85	7/1/2026 14:12	267.47	61.56	14.50	3.60	52.20	176.31
86	7/1/2026 14:15	267.89	60.90	14.49	3.81	55.21	179.00
87	7/1/2026 14:18	268.26	60.24	14.52	3.66	53.14	181.71
88	7/1/2026 14:21	268.63	59.57	14.43	3.40	49.06	184.26
89	7/1/2026 14:24	269.01	58.91	14.44	2.99	43.18	186.57
90	7/1/2026 14:27	269.38	58.24	14.43	2.53	36.51	188.56
91	7/1/2026 14:30	269.75	57.58	14.39	2.36	33.96	190.32
92	7/1/2026 14:33	270.09	56.92	14.44	2.39	34.51	192.04
93	7/1/2026 14:36	270.43	56.25	14.47	2.33	33.72	193.74

94	7/1/2026 14:39	270.76	55.59	14.43	2.29	33.04	195.41
95	7/1/2026 14:42	271.10	54.92	14.44	2.28	32.92	197.06
96	7/1/2026 14:45	271.44	54.26	14.46	2.32	33.55	198.72
97	7/1/2026 14:48	271.75	53.60	14.46	2.36	34.13	200.41
98	7/1/2026 14:51	272.07	52.93	14.41	2.30	33.14	202.09
99	7/1/2026 14:54	272.38	52.27	14.44	2.55	36.82	203.84
100	7/1/2026 14:57	272.70	51.60	14.40	3.14	45.22	205.89
101	7/1/2026 15:00	273.01	50.94	14.36	3.52	50.55	208.29
102	7/1/2026 15:03	273.31	50.28	14.36	3.77	54.14	210.91
103	7/1/2026 15:06	273.61	49.62	14.33	3.63	52.02	213.56
104	7/1/2026 15:09	273.90	48.95	14.33	3.32	47.58	216.05
105	7/1/2026 15:12	274.20	48.29	14.34	2.90	41.59	218.28
106	7/1/2026 15:15	274.50	47.63	14.37	2.43	34.92	220.19
107	7/1/2026 15:18	274.78	46.97	14.39	2.14	30.79	221.83
108	7/1/2026 15:21	275.07	46.31	14.28	2.08	29.70	223.35
109	7/1/2026 15:24	275.35	45.65	14.33	2.05	29.38	224.82
110	7/1/2026 15:27	275.64	44.99	14.28	2.15	30.70	226.33
111	7/1/2026 15:30	275.92	44.33	14.31	2.12	30.34	227.85
112	7/1/2026 15:33	276.20	43.67	14.28	2.04	29.13	229.34
113	7/1/2026 15:36	276.48	43.01	14.22	2.01	28.58	230.78
114	7/1/2026 15:39	276.75	42.35	14.30	2.05	29.32	232.23
115	7/1/2026 15:42	277.03	41.69	14.24	2.46	35.03	233.84
116	7/1/2026 15:45	277.31	41.03	14.23	3.08	43.83	235.81
117	7/1/2026 15:48	277.58	40.37	14.21	3.46	49.17	238.13

118	7/1/2026 15:51	277.85	39.71	14.21	3.71	52.72	240.68
119	7/1/2026 15:54	278.13	39.06	14.23	3.55	50.52	243.26
120	7/1/2026 15:57	278.40	38.40	14.20	3.24	46.01	245.67
121	7/1/2026 16:00	278.67	37.74	14.21	2.83	40.21	247.83

ANNEX-3

Hardware Assembly:

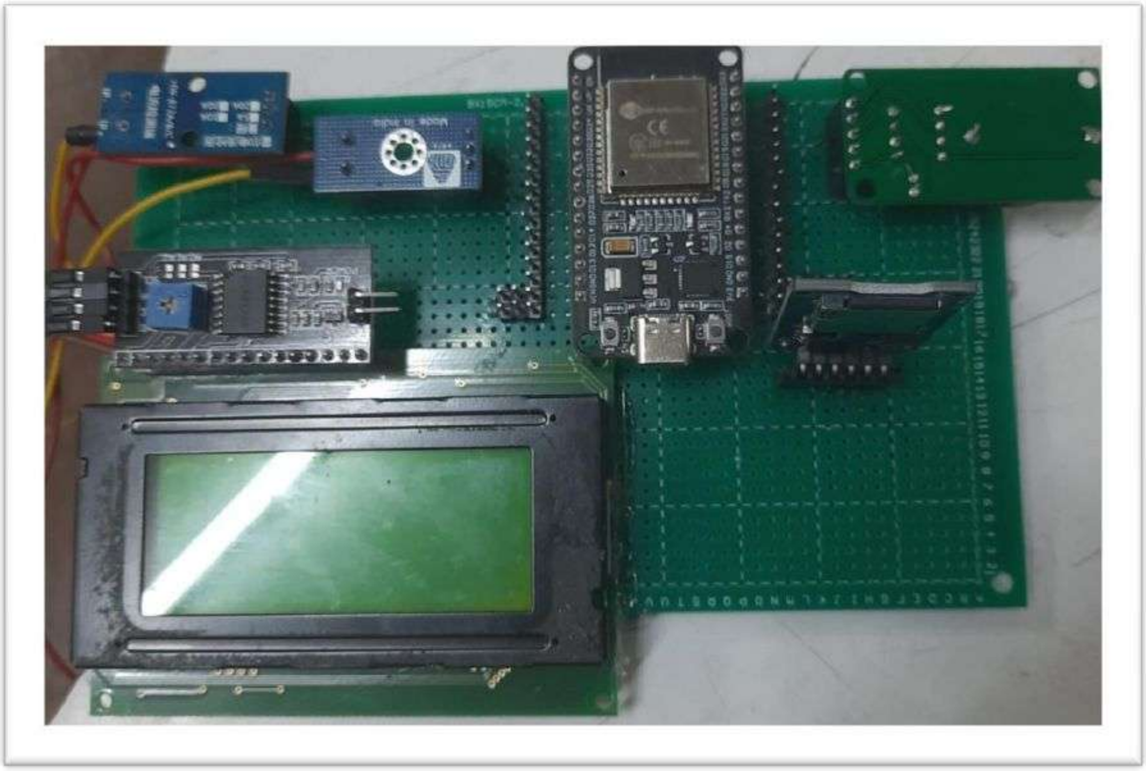

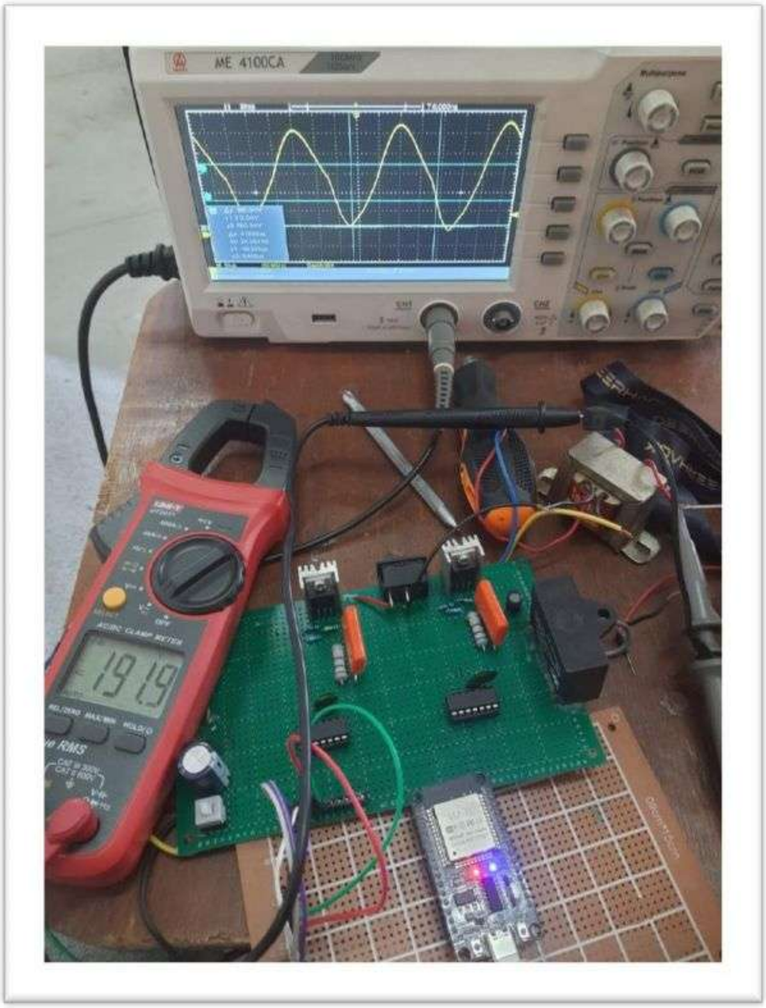
ME 4100CA
AC/DC CLAMP METER
1919

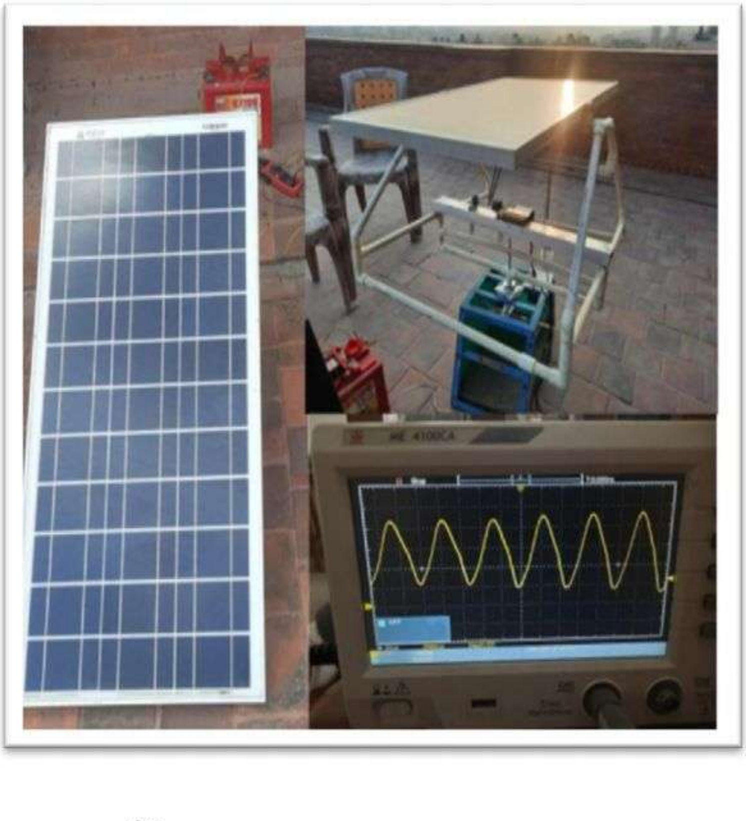
ME 4100CA

ANNEX-4

Development of Dual Tracker Mechanism:

ANNEX-5

Web Dashboard:

ANNEX-6

Circuit Diagram:

1. Inverter:

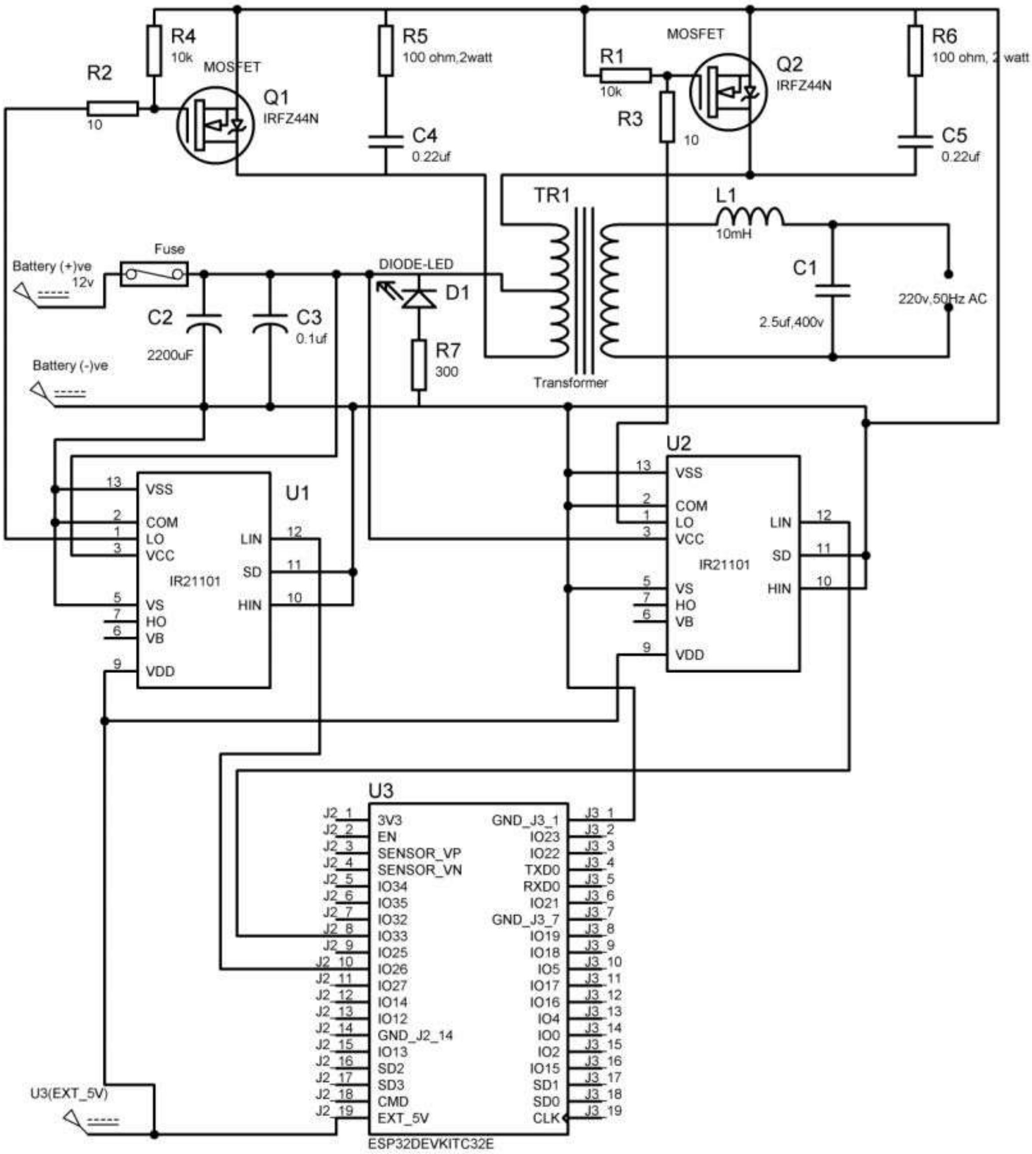

Inverter Circuit Diagram

2. Dual tracker motor and sensors:

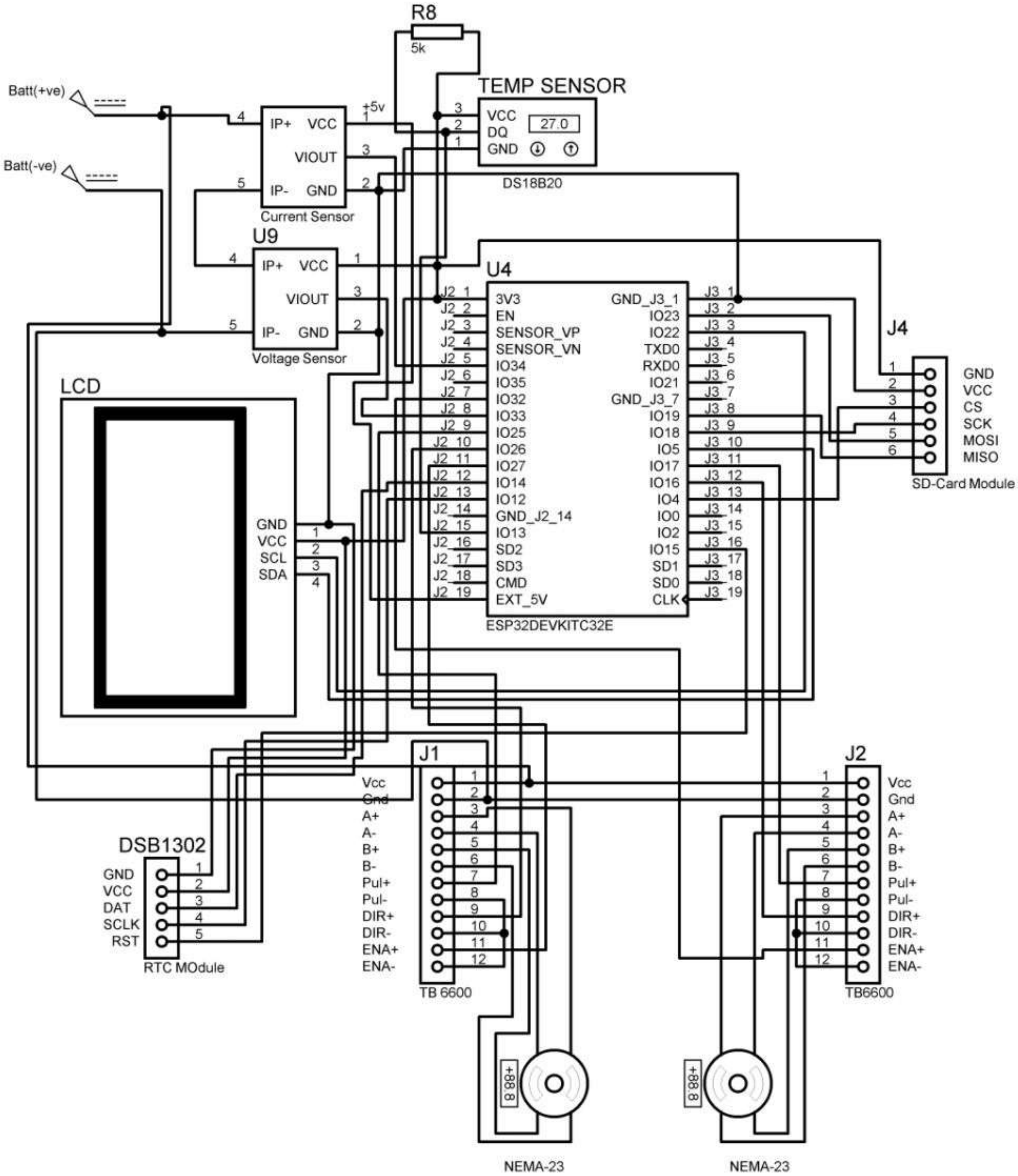

SCHEMATIC DIAGRAM